Finite Element Analysis of the Boom of Crane Loaded Statically

Bakr Noori Khudhur
Engineering College, University of Mosul /Mosul
Email: bakrnori@yahoo.com

Received on: 25/4/2012 & Accepted on: 10/1/2013

ABSTRACT

In this paper, the finite element analysis was carried out on boom of telescopic crane using ANSYS package software and the manual calculation as well as the analysis by the strength of materials procedure. The stress picture along the boom model was conducted under the maximum load carrying capacity. The stress developed at the interception of hydraulic rod with the first tube is higher than that developed along the rest of the boom. Moreover, the maximum deflection occurs at the boom head sheave.

In order to investigate the accuracy of the results, a comparison between the two approaches and the exact obtained by the strength of materials procedure is carried out.

Although the high capabilities of ANSYS software, the results are somewhat less accurate than that obtained by the manual calculations. Besides that, the results obtained by the finite element manual calculations are wholly similar to that of strength of materials procedure. Model taken for this paper is TADANO TR-350 XL 35-ton capacity.

Keywords: Stress, Static Loading, Boom, Crane, Finite Element, ANSYS.

التحليل بطريقة العناصر المحددة لذراع رافعة تلسكوبي تحت حمل ساكن

الخلاصة

في هذا البحث تم أجراء عملية تحليل للعناصر المحددة لذراع رافعة تلسكوبي (الذراع المتداخل) باستخدام برنامج إل (ANSYS)وبواسطة الحساب اليدوي بالإضافة إلى التحليل بواسطة طريقة مقاومة المواد. تم الحصول على صورة توزيع الأجهادات على طول الذراع تحت تأثير الأحمال القصوى ولوحظ أن أعظم الأجهادات تركزت في منطقة التقاء الذراع الهيدروليكي مع ذراع الرافعة. وبينت الدراسة أن أعظم انحراف حصل عند النهاية القصوى للذراع. لضمان صحة النتائج تمت مقارنة النتائج التي تم الحصول عليها من طريقتي التحليل بالعناصر المحددة مع النتائج الحقيقية من طريقة مقاومة المواد. بالرغم من الإمكانيات الكبيرة للبرنامج ألا أن النتائج التي تم الحصول عليها بواسطة هذا البرنامج كانت أقل دقة نوعا ما من تلك الناتجة بطريقة الحساب اليدوي. إلى جانب ذلك فان النتائج من الحساب اليدوي لطريقة العناصر المحددة كانت متطابقة كليا مع طريقة مقاومة المواد.

https://doi.org/10.30684/etj.2013.82179
2412-0758/University of Technology-Iraq, Baghdad, Iraq

INTRODUCTION

A crane is a lifting machine, generally equipped with a winder, wire ropes or chains and sheaves that can be used both to lift and lower materials and to move them horizontally. It uses one or more simple machines to create mechanical advantage and thus moves loads beyond the normal capability of human [1]. Cranes exist in enormous variety of forms. Each tailored to a specific use. Of these types, the telescopic crane is often used in Iraq and generally for short term construction projects. It is provided with a boom consists of tubes fitted one inside the other.

Zrnic, N. et al. [2] discussed the effect of moving loads to dynamic response of the crane boom structure as are deflections and bending moments. They focus on the interaction between trolley and supporting structure caused by the moving load. Gerdemely, I., et al. [3] calculated the strength of the tower crane parts according to finite element method and DIN standards and focused on prevention crane damage due to heavy loads. They calculated the stresses of the crane parts with ANSYS software considering the crane self weight, pay loads, hook weight and the dynamic loads. Langen, I. et al. [4] used numerical simulation of the dynamic behavior of the Norne offshore crane during lifting operation with the aid of FEDEM software program. They presented maximum dynamic stresses in deferent sections as a function of how the crane is operated in addition to the maximum load for various sea states to control the motion through power calculated. Mikkola, A. et al. [5] investigated the fatigue damage of a welded crane structure using ADAMA software in conjunction with ANSYS finite element software. The output information of ADAMA is used in the ANSYS program to determine a multiple load case. They calculated the stresses range occurrence and carry out a comparison between the model and the real structure to investigate the accuracy of the stress results.

This study concentrates on boom, since boom play an objective role in the load lifting operation and the maximum direct effect of the stress in initializing from it and effects to another attached assemblies of cranes.

The aim of this study is to investigate the stress distribution along the boom using finite element method with two approaches namely; the ANSYS package software and the manual calculations. The results are confirmed by a comparison made with the exact results obtained by strength of materials procedure. The results obtained by the manual calculations proved to be exact though it is carried out over a limited number of elements. Meanwhile, the ANSYS program demonstrated reasonable results. The stresses were shown highly concentrates around the attachment of the hydraulic rod with the boom.

BOOM MODEL DESCRIPTION

Model shown in Figure (1) represents boom of TADANO 35 ton. The telescopic boom has four tubes and the fourth one attached with boom head sheave. Load conditions taken in its full weight (30 ton) and maximum boom extension is 30 m.

The own weight of the boom is neglected as compared with the payload and this is possible as it neglected in both methods. The boom dimensions were measured and shown in Figure (1). The boom material is mild steel. With given boom parameters, the areas and area moment of inertias about z-axis were calculated and given in Table (1).

ANSYS ANALYSIS APPROACH

One of the main steps in the typical ANSYS analysis is the model generation that is done in the preprocessor. The boom of crane is modeled with solid modeling operation as hollow blocks with dimensions cited in Figure (1). The four blocks are generated and fitted one inside the other. Shell 63-four nodes was chosen as an appropriate element type for this model. The boom material properties are 206 GPA as Young modulus and Poisson's ratio of. The model $\nu = 0.3$ was meshed as shown in Figure (2).

The loads and boundary conditions were applied in solution processor according to Figure (1). Then the solutions were obtained for the model.

Finally the results were obtained over the entire of the model in General Postprocessor. The contour plots of the transverse deflection y, stresses in x and y-directions as well as the von Mises stress were obtained and shown in the Figure (3), Figure (4), Figure (5) and Figure (6) respectively.

FINITE ELEMENT ANALYSIS (MANUAL CALCULATION)

The boom is considered as a structural member carries transverse as well as axial loads and such members are known as beam- column. In the case of small deflection, the additional bending moment attributable to the axial loading is negligible.

For the present purpose, we assume the axial loads are such that these secondary effects are not of concern and the axial loading is independent of bending effect. This being the case, we can simply add the spar element stiffness matrix to the flexure element stiffness matrix to obtain the 6×6 element stiffness matrix for a flexure element with axial loading. The element equilibrium equations for such a combined form element can be [5].

$$[K^e]\{\delta^e\} = \{F^e\} \qquad ..(1)$$

Where, $[K^e]$ and $\{\delta^e\}$ are the $\{F^e\}$ element stiffness matrix, the displacement, and load vectors respectively.

The domain can be divided in to five sub domains and each one can be considered as a 2- node element. The elements and nodes are chosen and as shown in the bottom of Figure (7).

The individual element stiffness matrices were obtained (in equation (1)). For example, The element stiffness matrix for element number (1) is.

$$[K^{(1)}] = \begin{bmatrix} 3211.8 & 0 & 0 & -3211.8 & 0 & 0 \\ 0 & 156.54 & 399.17 & 0 & -156.54 & 394.18 \\ 0 & 399.17 & 1357.2 & 0 & -299.18 & 678.6 \\ -3211.8 & 0 & 0 & 3211.8 & 0 & 0 \\ 0 & -156.54 & -299.18 & 0 & 156.54 & -399.18 \\ 0 & 394.180 & 678.6 & 0 & -399.18 & 1357.2 \end{bmatrix} \; MN/m \quad [K]$$

The assembled system stiffness matrix, is obtained by the direct assembly procedure and the assembled system equations can be written as.

$$[K]\{\delta\} = F \qquad .... \quad (2)$$

Denoting the forces at node 1 as reaction components, owing to the displacement constraints $u_1 = v_1 = 0$. Taking the constraints in to account, the equations to be solved for the active displacements are be written as.

$$[K']\{\delta'\}=F' \quad .... \quad (3)$$

Where $[K']$ is the active system stiffness matrix , $\{\delta'\}$ is the active displacement vector, and $[F']$ is the active force vector.
The explicit forms of equation 1, 2, and 3 are written in the Appendix A.

The numerical results for these equations are obtained via the computer software MATLAB give the displacement values as shown in Table (2)

Once the deflections have been determined, the stresses are easily found [4]

$$\{\sigma\} = [D]\,[B]\,\{\delta\} \quad \ldots (4)$$

$$=\frac{-yE}{l^2}[-6+12\zeta \quad l(6\zeta-4) \quad 6-12\zeta \quad l(6\zeta-2)]\ \{\delta\}$$

Where $[D]$ is the modulus matrix, $[B]$ is the strain displacement matrix, is the y distance from the neutral axis to the top fiber, and is ζ dimensionless factor and equal to x/l .

To avoid the differences in stress computation at the juncture of two adjusting elements. The stresses are calculated at anywhere else other than the nodes. For element 1 as a sample of stress calculation:

$$\sigma=\frac{-yE}{l^2}[0 \quad -1 \quad 0 \quad 1]\{\delta\}$$

$$\sigma=\frac{-yE}{l^2}(\theta_2-\theta_1) \quad ... \quad (5)$$

Noting that for cross section of the element 1 , y max = 0.41 m

$$\sigma=\frac{-0.41\times 206\times 10^9}{5.1^2}(-0.0043656-0.0023244)$$

$$\sigma = 45.72 \quad MPa \quad tension$$

And the axial stress is given by

$$\sigma=\frac{E}{l}(u_2-u_1). \quad .... \quad (6)$$

$$\sigma_{axial}=\frac{206\times 10^9}{5.1}(0.0010919-0)$$

$$\sigma_{axial}=44.1 \quad MPa \quad tension$$

The stress computation must take into account the superposition of bending stress and direct axial stress and is computed by the tensile axial stress added to the tensile portion of the bending stress (at the top fiber) to give

$$\sigma = 99.82 \quad MPa \quad tension$$

The bending, axial and combined stresses are calculated and given as shown in Table (3).

STRENGTH OF MATERIALS PROCEDURE

Having the angle α is given to be 7.06° the equilibrium conditions for the entire boom yields (per the top of Figure (8).

$$A_x = -3506.3\ kN$$
$$A_y = -366.9\ kN$$
$$F_x = 3569.33\ kN$$
$$F_y = 442.053\ kN$$

Resolving the load at H into x and y directions gives

$$H_x = -63.06\ kN$$
$$H_y = -75.15\ kN$$

The problem of solving deflections and stresses carried out using strength of materials calculations via bending moments and shearing force diagrams. The plot of S.F. and B.M. diagrams is shown in Figure (8).

Since both methods give the stresses at the same coordinate x to compute their characteristics, appropriate points along the x-axis were determined as 0.0, 2.55, 6.3, 11.25, 18.75, 26.25 and 30 m.

The bending moments at the foregoing sections are found and the corresponding bending stresses are calculated using the formula $\sigma = \frac{M\,y}{I}$.

At x = 2.55 m, the bending moment is - 935.6 kN.m. Because M is negative, the maximum tensile stress occurs at the top fiber.

$$\sigma = \frac{935.6 \times 0.41}{8.4 \times 10^{-3}} = 45.67 \quad MPa \quad tension$$

The axial stress at x = 2.55 m is thus

$$\sigma = \frac{3506.27}{0.0795} = 44100\ \ kPa$$
$$or\ \ 44.1\ \ MPa \quad tension$$

Superimposing the two stresses, we obtain the greatest tensile stress of the section at the top fiber [6].

$$\sigma = 45.67 + 44.1 = 99.77\,MPa\ \ tension$$

For each section x, Bending moments $B.M$, the corresponding bending tress σ_b , axial stress σ_a and the combined stress σ_c are calculated and listed in Table (4).

RESULTS

By using the finite element method, the deflection and stress are obtained along the boom. The general purpose finite element program ANSYS is used to obtain the stress picture along the boom of the crane under the condition of static loading and boundary conditions set from the adopted model.

Figure (3) shows the transverse deflection of the boom. It is obvious that the maximum deflection is occurred at the tip of the boom and this seems reasonable since it is the point at which the load is lifted. However, the deflection decreases down the tip of the boom.

A good picture of stress distribution is obtained along the boom via the contour plots of axial and transverse stresses as shown in Figure (4) and Figure (5) respectively. In this connection, it is clearly shown that the maximum stress induced in the boom is at the interception of hydraulic rod with the boom. Unlike that, the stress developed at the ends are so small whereas most of the rest of the boom is considered as low stress region.

Figure (6) demonstrates the von Mises stress along the boom. It is imported to note that the maximum value reported is 832 MPa which is much less than the yield stress of the boom materials.

Having seen the maximum deflection is occurred at the boom head sheave, the deflection is positive in the first tube and changes in to negative in the following tubes as shown in Figure (9). However, this is somehow unclear in ANSYS solution. Zero deflections occur at the juncture of first tube with the second.

The two approaches of finite Element Solution are confirmed by plotting their calculated stress with that obtained by Strength of Materials procedure Figure (10). It was consistently found that the manually calculated FEM yields very close results to the strength of materials procedure and delivers the same convergent solution but there are some discrepancies with ANSYS results. Therefore, exact solution is achieved with manual calculations though the FEA is an approximate method. This is due to the fact that the deflection equation of the neutral surface is a cubic equation as well as the interpolation functions.

CONCLUSIONS

The three approaches reveal that the maximum deflection occurs at the boom head sheave and the maximum stresses concentrates at the interception of the hydraulic road with the boom.

Sometimes exact solution can be achieved by the finite element analysis though it is an approximate.

By choosing the shell element and analyzing with the ANSYS software package, various and detailed results can be listed and plotted but exact results couldn't be accessed. In this problem exact solution is achieved by the manual calculation of finite element analysis and by the strength of material procedure as well.

REFERENCES

[1]. Zrink, N., D. Oguamanam, and S. Bosnjak, "Dynamic and Modeling of mega quayside container cranes", FME transactions, Vol. 34, No. 4, 2004, pp. 193-198.

[2].WikimediaFoundationWebsite.Retrieved2011,from:http://en.Wikipedia.org/wiki/crane (machine).

[3]. Gerdemely, I., S. Kurt, and O. Deliktas "Finite element analysis of the tower crane",14th International Research/ Expert Conference, Trends in the Development Machinery and Associated Technology" TMT 2010, Mediterranean Cruise, 11-18 Sept. 2010.

[4]. Langen, I. and Th. Kim Than "Simulation of dynamic behavior of a FPSO crane", Retrieved (2011), from :http//trac.no/download/crane_pap-er.

[5]. Mikkola, A., H. Handroos, and E. Niemi "Using ADAMS simulation for predicting dynamic force histories for the fatigue analysis of a log crane", Retrieved(2011),availableat:http//mscsoftware.com/support/limbrary/conf/adams/…uc960011.pd.
[6]. Desai, C.S., and J.F. Abel. Introduction to the Finite Element Method. New York: Van Nostrand Reinhold, 1972.
[7]. Zienkiewics, O.C., and R.L. Taylor. The Finite Element Method , 4th ed. London: McGraw-Hill, 1977.
[8]. Ugural, A.C. Mechanics of Materials, New York: McGraw-Hill, 1991.
[9]. Liu, G.R., and S.S. Quek. The Finite Element Method: A Practical Course, Oxford: Butterworth-Heinemann.
[10]. Hutton, David V. Fundamentals of finite Element Analysis, 1st ed. New York: McGraw-Hill, 2004.
[11]. Xianuan, Zang, et al. (2010) " Finite element analysis and optimization of the telescopic arm of a 160-ton rai way rescue crane" Retrieved 3011 From: http://en.cnki.com.cn/Article_en/CJFDTOTAL-QZJJ20.

Table (1) Areas and area moment of inertias.

Tube	Length (L),m	Area (a), m^2	Moment of Inertia (I), m^4
AB	7.5	0.0795	8.4
BC	7.5	0.1029	9.3
CD	7.5	0.0931	6.9
DE	7.5	0.0833	4.9

Table (2) Displacement values in meters calculated manually at the nodes.

δ	values	δ	values	δ	values	δ	Values
θ_1	0.0023244	u_3	0.0010806	v_4	-0.040909	θ_5	- 0.012049
u_2	0.0010919	v_3	0.0030911	θ_4	-0.008451	u_6	0.0010081
v_2	0.0071605	θ_3	- 0.0029133	u_5	0.0010356	v_6	- 0.23082
θ_2	-0.00043656	u_4	0.0010603	v_5	-0.12299	θ_6	- 0.015095

Table (3) Bending, axial, and combined stresses along the boom calculated by FEM.

x, m	$y_{\max}, m$	σ_b, MPa	σ_{axial}, MPa	σ_c, MPa
0	0.41	0	44.1	44.1
2.55	0.41	45.72	44.1	99.82
6.3	0.41	87.16	-0.8	86.36
11.25	0.385	58.16	-0.61	57.55
18.75	0.35	43.24	-0.68	42.56
26.25	0.315	18.57	-0.76	17.81
30	0.315	0	-0.76	-0.76

Table (4) bending moments, bending stresses, axial stresses and combined stresses along the boom.

x, m	$B.M, kN.m$	σ_b, MPa	σ_a, MPa	σ_c, MPa
0	0	0	44.1	44.1
2.55	-935.6	45.67	44.1	99.77
6.3	-1781.1	86.94	-0.79	86.15
11.25	-1409.33	58.34	-0.61	57.13
18.75	-846.1	42.92	-0.677	42.243
26.25	-282.83	18.18	-0.757	17.423
30	0	0	-0.757	-0.757

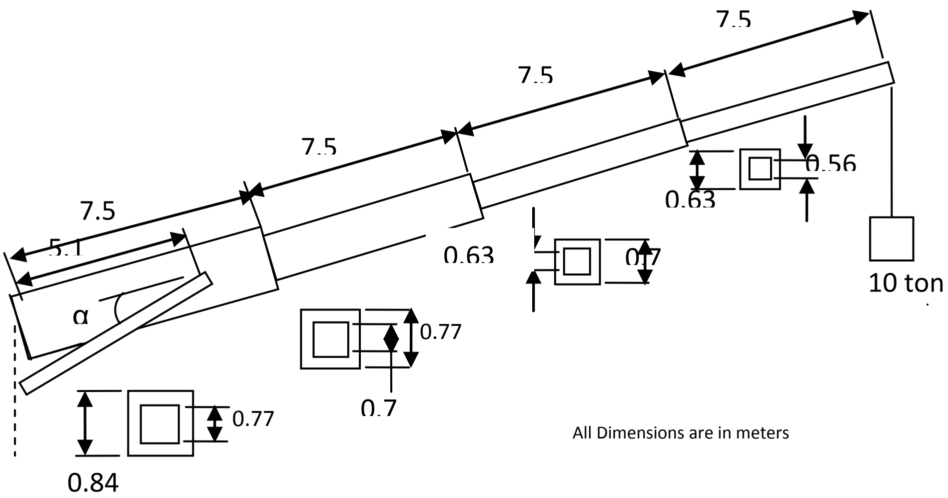

Figure (1) Boom model dimensions.

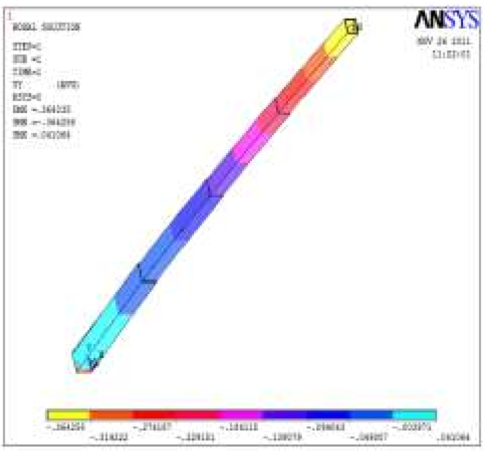

Figure (2) Finite element model of boom.

Figure (3) the transverse deflection.

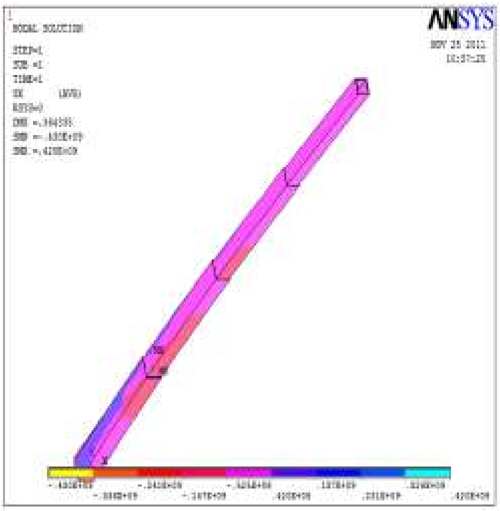

Figure (4) the axial stress.

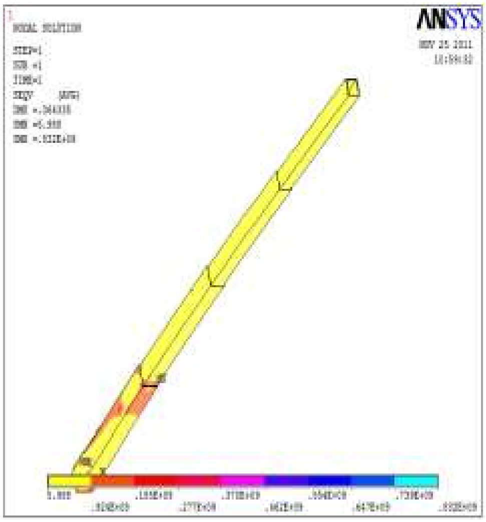

Figure (5) the transverse stress.

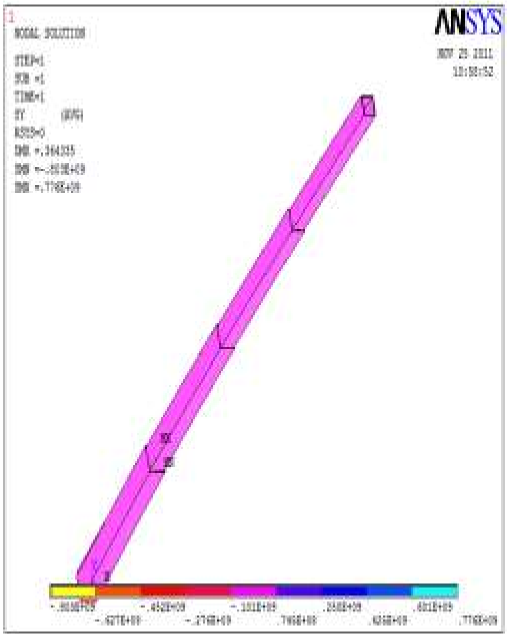

Figure (6) The von Mises stress.

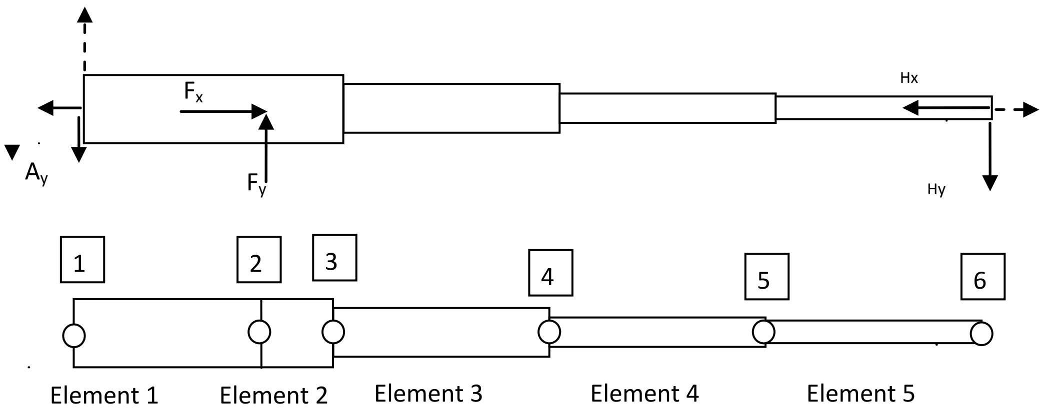

Figure (7) The Boom descretized into elements.

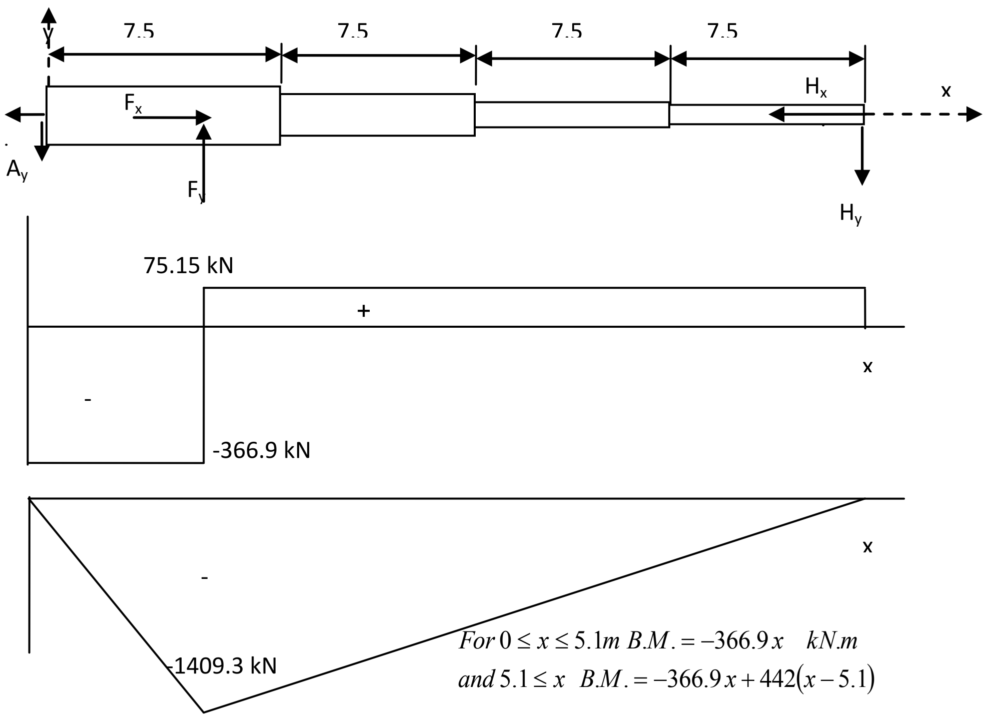

Figure (8) Shearing force and bending moments diagrams.

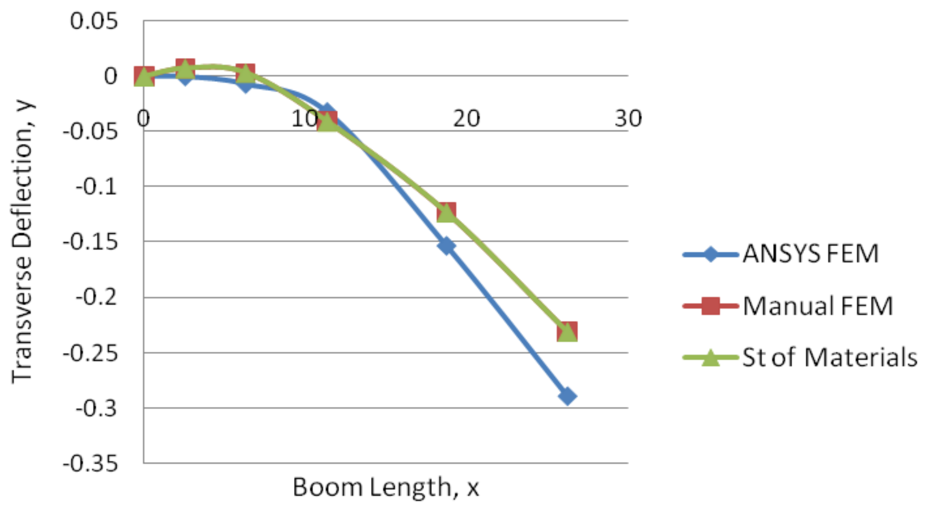

Figure (9) Transverse deflection along the boom length.

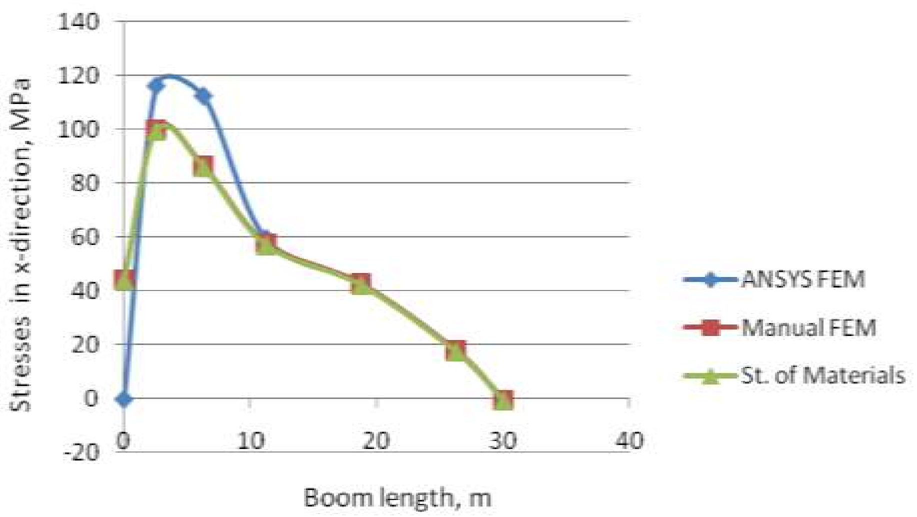

Figure (10) Stresses along the boom length calculated in x-direction.

Appendix A

The explicit form of equations 1, 2, and 3 are

$$\begin{bmatrix} aE/l & 0 & 0 & -aE/l & 0 & 0 \\ 0 & 12EI/l^3 & 6EI/l^2 & 0 & -12EI/l^3 & 6EI/l^2 \\ 0 & 6EI/l^2 & 4EI/l & 0 & -6EI/l^2 & 2EI/l \\ -aE/l & 0 & 0 & aE/l & 0 & 0 \\ 0 & -12EI/l^3 & -6EI/l^2 & 0 & 12EI/l^3 & -6EI/l^2 \\ 0 & 6EI/l^2 & 2EI/l & 0 & -6EI/l^2 & 4EI/l \end{bmatrix} \begin{Bmatrix} u_i \\ v_i \\ \theta_i \\ u_j \\ v_j \\ \theta_j \end{Bmatrix} = \begin{Bmatrix} Q_i \\ V_i \\ M_i \\ Q_j \\ V_j \\ M_j \end{Bmatrix} \quad \text{........} \quad (1)$$

$$[K]\begin{Bmatrix} u_1 \\ v_1 \\ \theta_1 \\ u_2 \\ v_2 \\ \theta_2 \\ u_3 \\ v_3 \\ \theta_3 \\ u_4 \\ v_4 \\ \theta_4 \\ u_5 \\ v_5 \\ \theta_5 \\ u_6 \\ v_6 \\ \theta_6 \end{Bmatrix} = \begin{Bmatrix} A_x \\ A_y \\ 0 \\ 3.596\times10^6 \\ 0.442\times10^6 \\ 0 \\ 0 \\ 0 \\ 0 \\ 0 \\ 0 \\ 0 \\ 0 \\ 0 \\ 0 \\ -63\times10^3 \\ -75.15\times10^3 \\ 0 \end{Bmatrix} \quad \text{..} \quad (2)$$

$$[K']\begin{Bmatrix} \theta_1 \\ u_2 \\ v_2 \\ \theta_2 \\ u_3 \\ v_3 \\ \theta_3 \\ u_4 \\ v_4 \\ \theta_4 \\ u_5 \\ v_5 \\ \theta_5 \\ u_6 \\ v_6 \\ \theta_6 \end{Bmatrix} = \begin{Bmatrix} 0 \\ 3.596\times10^6 \\ 0.442\times10^6 \\ 0 \\ 0 \\ 0 \\ 0 \\ 0 \\ 0 \\ 0 \\ 0 \\ 0 \\ 0 \\ -63\times10^3 \\ -75.15\times10^3 \\ 0 \end{Bmatrix} \quad \text{...} \quad (3)$$

Where the elements of the system stiffness matrix, $[K]$ are written as:

$$\begin{bmatrix}
3211 & 0 & 0 & -3211 & 0 & 0 & 0 & 0 & 0 & 0 & 0 & 0 & 0 & 0 & 0 & 0 & 0 & 0 \\
0 & 156 & 399 & 0 & -156 & 394 & 0 & 0 & 0 & 0 & 0 & 0 & 0 & 0 & 0 & 0 & 0 & 0 \\
0 & 399 & 1378 & 0 & -399 & 678 & 0 & 0 & 0 & 0 & 0 & 0 & 0 & 0 & 0 & 0 & 0 & 0 \\
-3211 & 0 & 0 & 100135 & 0 & 0 & -6824 & 0 & 0 & 0 & 0 & 0 & 0 & 0 & 0 & 0 & 0 & 0 \\
0 & -156 & -399 & 0 & 1658 & 1403 & 0 & -1502 & 1802 & 0 & 0 & 0 & 0 & 0 & 0 & 0 & 0 & 0 \\
0 & 394 & 678 & 0 & 1403 & 4241 & 0 & -1802 & 1442 & 0 & 0 & 0 & 0 & 0 & 0 & 0 & 0 & 0 \\
0 & 0 & 0 & -6824 & 0 & 0 & 9650 & 0 & 0 & -2826 & 0 & 0 & 0 & 0 & 0 & 0 & 0 & 0 \\
0 & 0 & 0 & 0 & -1502 & -1802 & 0 & 1556 & -1598 & 0 & -54 & 204 & 0 & 0 & 0 & 0 & 0 & 0 \\
0 & 0 & 0 & 0 & 1802 & 1441 & 0 & -1598 & 3906 & 0 & -204 & 510 & 0 & 0 & 0 & 0 & 0 & 0 \\
0 & 0 & 0 & 0 & 0 & 0 & -2826 & 0 & 0 & 5384 & 0 & 0 & -2557 & 0 & 0 & 0 & 0 & 0 \\
0 & 0 & 0 & 0 & 0 & 0 & 0 & -54 & -204 & 0 & 94 & -52 & 0 & -40 & 151 & 0 & 0 & 0 \\
0 & 0 & 0 & 0 & 0 & 0 & 0 & 204 & 510 & 0 & -52 & 1780 & 0 & -151 & 379 & 0 & 0 & 0 \\
0 & 0 & 0 & 0 & 0 & 0 & 0 & 0 & 0 & -2557 & 0 & 0 & 4845 & 0 & 0 & -2288 & 0 & 0 \\
0 & 0 & 0 & 0 & 0 & 0 & 0 & 0 & 0 & 0 & -40 & -152 & 0 & 69 & -43 & 0 & -28 & 107 \\
0 & 0 & 0 & 0 & 0 & 0 & 0 & 0 & 0 & 0 & 151 & 379 & 0 & -43 & 1296 & 0 & -108 & 269 \\
0 & 0 & 0 & 0 & 0 & 0 & 0 & 0 & 0 & 0 & 0 & 0 & -2288 & 0 & 0 & 2288 & 0 & 0 \\
0 & 0 & 0 & 0 & 0 & 0 & 0 & 0 & 0 & 0 & 0 & 0 & 0 & -28 & -107 & 0 & 28 & -108 \\
0 & 0 & 0 & 0 & 0 & 0 & 0 & 0 & 0 & 0 & 0 & 0 & 0 & 107 & 269 & 0 & -108 & 538
\end{bmatrix}$$

And the elements of the active system stiffness matrix, $\left[K^{'}\right]$ are written as:

$$\begin{bmatrix}
1378 & 0 & -399 & 678 & 0 & 0 & 0 & 0 & 0 & 0 & 0 & 0 & 0 & 0 & 0 & 0 \\
0 & 10035 & 0 & 0 & -6824 & 0 & 0 & 0 & 0 & 0 & 0 & 0 & 0 & 0 & 0 & 0 \\
-399 & 0 & 1658 & 1403 & 0 & -1502 & 1802 & 0 & 0 & 0 & 0 & 0 & 0 & 0 & 0 & 0 \\
678 & 0 & 1403 & 4241 & 0 & -1802 & 1442 & 0 & 0 & 0 & 0 & 0 & 0 & 0 & 0 & 0 \\
0 & -6824 & 0 & 0 & 9650 & 0 & 0 & -2826 & 0 & 0 & 0 & 0 & 0 & 0 & 0 & 0 \\
0 & 0 & -1502 & -1802 & 0 & 1556 & -1598 & 0 & -54 & 204 & 0 & 0 & 0 & 0 & 0 & 0 \\
0 & 0 & 1802 & 1441 & 0 & -1598 & 3906 & 0 & -204 & 510 & 0 & 0 & 0 & 0 & 0 & 0 \\
0 & 0 & 0 & 0 & -2826 & 0 & 0 & 5384 & 0 & 0 & -2557 & 0 & 0 & 0 & 0 & 0 \\
0 & 0 & 0 & 0 & 0 & -54 & -204 & 0 & 94 & -52 & 0 & -40 & 151 & 0 & 0 & 0 \\
0 & 0 & 0 & 0 & 0 & 204 & 510 & 0 & -52 & 1780 & 0 & -151 & 379 & 0 & 0 & 0 \\
0 & 0 & 0 & 0 & 0 & 0 & 0 & -2557 & 0 & 0 & 4845 & 0 & 0 & -2288 & 0 & 0 \\
0 & 0 & 0 & 0 & 0 & 0 & 0 & 0 & -40 & -152 & 0 & 69 & -43 & 0 & -28 & 107 \\
0 & 0 & 0 & 0 & 0 & 0 & 0 & 0 & 151 & 379 & 0 & -43 & 1296 & 0 & -108 & 269 \\
0 & 0 & 0 & 0 & 0 & 0 & 0 & 0 & 0 & 0 & -2288 & 0 & 0 & 2288 & 0 & 0 \\
0 & 0 & 0 & 0 & 0 & 0 & 0 & 0 & 0 & 0 & 0 & -28 & -107 & 0 & 28 & -107 \\
0 & 0 & 0 & 0 & 0 & 0 & 0 & 0 & 0 & 0 & 0 & 107 & 269 & 0 & -108 & 538
\end{bmatrix}$$